[AMERICAN JOURNAL OF SCIENCE, VOL. 288, OCTOBER, 1988, P. 777-797]

American Journal of Science

OCTOBER 1988

MASS-TRANSPORT CONSTRAINTS ON THE GROWTH OF DISCOIDAL FERROMANGANESE NODULES

BERNARD P. BOUDREAU*

Department of Oceanography, University of British Columbia, Vancouver, British Columbia, Canada V6T 1W5

ABSTRACT. Because presently available data suggest that the coarse-grained sediments found usually beneath shallow-water ferromanganese nodules are unlikely to support substantial fluxes of dissolved metals, the common discoidal morphology of these nodules cannot be ascribed generally to the action of an underlying diagenetic source. Grill (1978) has advanced that lateral movement of metal-enriched bottom waters supplies the needed metals. Based on this hypothesis, a growth model is formulated using boundary-layer transport theory and linear precipitation kinetics at the nodule surface. The model reproduces not only the discoidal morphology but also predicts growth-rates in order-of-magnitude agreement with those inferred from independent methods. The success of the present model argues that the discoidal morphology of these nodules is a result of the marked contrast in metal fluxes between sediment and nodule surfaces; that is to say, a nodule is a strong sink whereas the sediment is a weak sink or a source for metals. The theory also provides a general framework to explain the morphology and, perhaps, the growth rates of all nodules, including those of the deep sea.

INTRODUCTION

Although most scientific attention has focused on their deep-sea brethren, ferromanganese nodules are also found on the floors of temperate shallow seas and lakes (Murray and Irvine, 1894; Manheim, 1965; Price, 1967; Callender and Bowser, 1976; Calvert and Price, 1977; Dean and Ghosh, 1981). The morphology of these nodules is varied, but two dominant endmembers are easily identified: spherical nodules and flat, discoidal nodules or girdles of oxide around rock nuclei (Calvert and Price, 1977).

The reigning paradigm to explain the formation of these nodules holds that these two shapes reflect different sources of metals (Manheim, 1965). Discoidal nodules and girdles are found where the supply of metals is dominantly from the underlying sediments as a result of diagenetic remobilization (Manheim, 1965; Price, 1967; Callender and Bowser, 1976; Calvert and Price, 1977; Winterhalter, 1981). Spherical

* Present address: Department of Oceanography, Dalhousie University, Halifax, Nova Scotia, Canada B3H 4J1.

nodules are thought to occur on more oxidized sediments, where bottom water acts as the main source of metals (Manheim, 1965).

However, the solid composition and porewater geochemistry of sediments associated with nodules from shallow seas and lakes are inconsistent with this formational theory. Discoidal nodules are found most commonly on coarse-grained sediments, such as sands (Harris and Troup, 1970; Sozanski and Cronan, 1976; Calvert and Price, 1977; Dean and Ghosh, 1981) and, far less frequently, on firm glacial clays. These sediments are characteristic of high-energy environments, typically well oxygenated, poor in organic matter, and, hence, questionable diagenetic sources of metals.

Indeed, Varentsov (1973) calculated that the thin post-glacial clays in the Gulf of Riga cannot have supplied the amount of metals in the nodules resting on these sediments. Kepkay (1985), upon measuring dissolved Fe and Mn in the porewaters of sediments underlying a field of discoidal nodules in Lake Charlotte, Nova Scotia, found that the diffusive flux of these metals is directed into the sediments from the lake waters. Moreover, there is little evidence of significant metal oxide accretion on the underside of discoidal nodules (Sozanski and Cronan, 1976). Conversely, the nodules found on and within fine-grained, organic-matter bearing sediments of shallow seas and lakes are usually spherical (Calvert and Price, 1977).

A more consistent growth theory for discoidal shallow-water nodules can be developed by considering the geological setting and hydrodynamic properties of their environment. This paper proffers such a theory.

THE MODEL

Discoidal nodules accrete at the sediment interface (Dean and Ghosh, 1981). Grill (1978) shows that the bottom water flowing laterally over these nodules can be enriched in diagenetically remobilized metals derived from fine-grained sediments in other parts of shallow seas or lakes and goes on to suggest that this water acts as the source of metals for nodule growth. This paper advances the proposition that Grill (1978) is correct in his proposal and that the rate of growth and the morphology of these nodules result from the peculiarities of the mass-transport processes between the nodule surface and the bottom water.

To understand this last claim, an examination of some aspects of boundary-layer theory is required. Incidentally, this exposition should also dispel some misconceptions that have arisen about the validity of classical boundary-layer theory in view of the discovery of turbulent "bursts." This presentation is necessarily cursory, and I refer the reader to extensive reviews by Schlichting (1968), Hinze (1975), Sideman and Pinczewski (1975), and Boudreau and Guinasso (1982) for missing details.

Boundary-layer preliminaries.—Consider the simple case of momentum and mass transfer between a flat solid interface of infinite extent and a fluid flowing along this surface. This classical problem has been studied exhaustively by fluid dynamicists and chemical engineers. Their extensive measurements of the velocity profile in the fluid adjacent to such a plate have established a number of empirical *facts* that are independent of any theory employed to explain them.

Foremost among these is that the time-averaged velocity profile is dynamically similar under all fully-turbulent conditions; that is to say, if the tangential component of the velocity, u, at each height above the plate, z, is scaled to the shear velocity, u_*, and plotted against the dimensionless height, u_*z/ν ($\nu \equiv$ kinematic viscosity), then all turbulent flows produce the same profile, called the law of the wall (fig. 1). In particular, the velocity in the lower portion of this profile, $u_*z/\nu \leq 7$, is well represented by

$$\frac{u}{u_*} = \frac{u_*z}{\nu} \tag{1}$$

which holds for geophysical flows (Chriss and Caldwell, 1984).

The linearity of eq (1) suggested to some early researchers that the flow in the zone $zu_*/\nu \leq 7$ was laminar. It also gave birth to the classical

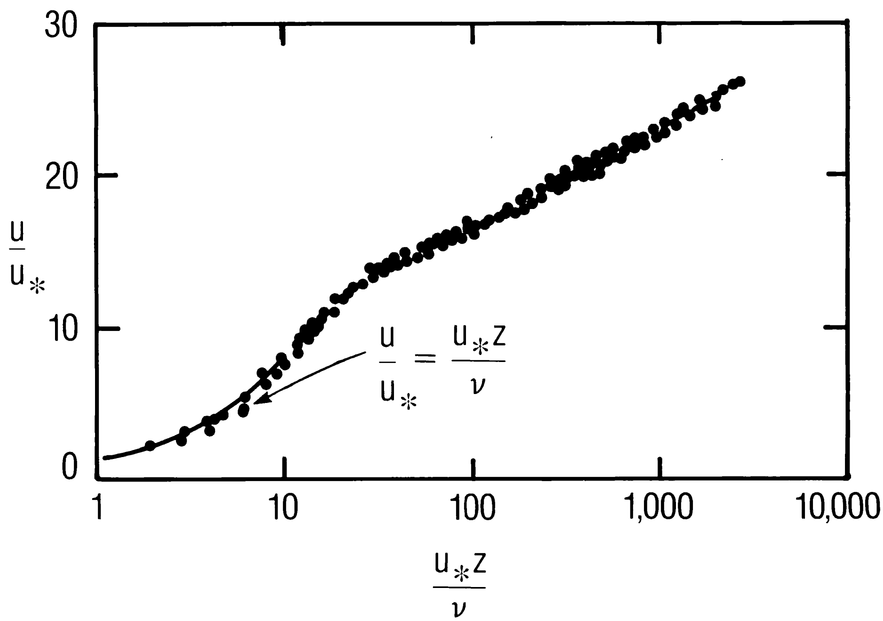

Fig. 1. Universal, dimensionless, time-averaged velocity profile measured by Deissler (1951). The region of linear flow, eq (1), extends to about $u_*z/v \simeq 7$. This is the lower portion of the traditional viscous sublayer. The diffusive sublayer constitutes about the lower one-tenth of this region.

theory for boundary layers, which holds, that within the zone of validity of eq (1), momentum transfer is dominated by molecular viscosity, hence the name viscous sublayer. Above this zone, viscous dampening is ineffective at suppressing turbulence, and momentum transport is accomplished by eddies.

This mechanistic picture has proven to be inaccurate. As early as 1932, Fage and Townsend showed that the instantaneous flow in this layer is not laminar, and careful writers employed the term linear to describe the time-averaged flow. The classical notions have been rocked further by the flow visualization experiments conducted by Kline and others (1967), Corino and Broadkey (1969), and many others since. These investigations found that the flow in the lower boundary layer is formed by a mosaic of rolling motions periodically disrupted by violent movements called bursts. The frequency of these bursts decreases significantly as the plate surface is neared.

These discoveries are not license, however, to discard or reject the empirical findings of the old boundary-layer theory, including eq (1). When the velocity measurements made while studying intermittent behavior such as bursts are time-averaged, they do indeed produce profiles consistent with the law of the wall and eq (1) in particular (for example, Kline and others, 1967; Grass, 1971; Blackwelder and Haritonidis, 1983; Willmarth and Sharma, 1984).

The classical boundary-layer theory and one based on periodic interruptions by bursts are not incompatible. To quote Sideman and Pinczewski (1975, p. 51):

> "Although it may first appear that there is little in common between the approach based on the classical concept of an eddy transport coefficient and that based on the concept of surface renewal [bursts], the two concepts are by no means mutually exclusive. Rather, we may consider the former to represent a macro-scale study of the phenomena while the latter is a micro-scale analysis limited to the viscous transport region. In a sense, these two approaches are complementary." [my addition in brackets]

Even more to the point, Davies (1977, p. 7) states that

> ". . . the 'bursts' of fluid are physically the 'lumps' of fluid envisaged in the eddy-mixing length theory of mean eddy diffusivities."

Therefore, the bursting phenomenon supplies mechanistic understanding of momentum (and mass) transfer, but it does not negate past work, nor does it mean that it is improper to employ classical theory when the time scale of interest is much longer than the period of a few bursting events (a few hundred seconds at most, Blackwelder and Haritonidis, 1983). As remarked earlier by Townsend (1956), the concept of transport by means of an eddy diffusion is useful in that it yields a successful description of the mean momentum distribution, although it bears little resemblance to the actual physical processes taking place.

The classical (eddy) boundary-layer model for mass transfer holds that, in analogy to momentum transport, there is a thin layer of fluid adjacent to the plate in which molecular diffusion dominates over eddy mixing (the diffusive sublayer). As molecular diffusion coefficients, D, are typically many orders of magnitude smaller than the kinematic viscosity of water ($\nu/D \simeq 1000$ in seawater, Boudreau and Guinasso, 1982), the diffusive sublayer is buried deep within the viscous sublayer where eq (1) is valid.

If the infinite plate considered above is also a spatially-uniform chemical sink for a trace constituent of the flowing fluid, then the classical approach suggests that the mass flux, J, across the boundary layer is correlated to the difference between the concentration in the turbulent fluid, C_∞, and that at the interface, C_o,

$$J = \beta\,(C_\infty - C_o) \tag{2}$$

where the correlation function, β, called the mass-transfer coefficient, depends on the hydrodynamic and chemical properties of the flow (that is u_*, ν, and the diffusion coefficient of the species in question, D). This functionality is determined empirically from measurements of the ratio $J/[(C_\infty - C_o)u_*]$ and is found to be "universally self-similar," like the velocity profile. We can also define the formal thickness of the diffusive sublayer, δ, as D/β.

In the light of the discovery of bursting, what is the relevance of eq (2)? Not surprisingly, it retains all its old value because it is empirical. Again, bursting supplies a way of understanding the instantaneous processes of mass transport, while eddy diffusivity and mass-transfer coefficients remain useful time-averaged devices.

Two observations lend support to this statement. First, a comparison of a mass-transfer correlation from a bursting model and that from classical boundary-layer theory shows that they provide similar results. Specifically, Sideman and Pinczewski (1975) use a periodic boundary-layer model to obtain the mass-transfer coefficient between bursts, β',

$$\beta' = 0.678\left[\frac{D^2u_*}{t\nu}\right]^{1/3} \tag{3A}$$

where t is the time since the last burst. Averaged over the period from the last burst and inclusive of the next burst, they obtained for a mean mass-transfer coefficient

$$\beta = 0.0671\ u_*\left[\frac{D}{\nu}\right]^{2/3} \tag{3B}$$

Meanwhile, Shaw and Hanratty (1977) take a classical approach and obtain the result

$$\beta = 0.0899\ u_*\left[\frac{D}{\nu}\right]^{0.704} \tag{4}$$

For dissolved Mn under the conditions of interest in temperate lakes (for example, $D = 5.75 \cdot 10^{-6}\ cm^2\ sec^{-1}$, $\nu = 10^{-2}\ cm^2\ sec^{-1}$, and $u_* = 1.0$ cm sec^{-1}), eqs (3B) and (4) differ by about 1 percent.

Secondly, the classical approach continues to be used (for example, Shaw and Hanratty, 1977; Sandall, Hanna, and Mazet, 1980) even while some of these same authors publish results on intermittent boundary layers (for example, Campbell and Hanratty, 1983a,b). The duality in the description of mass transfer is both well established and useful.

Application to nodules.—The mass-transfer process to nodules on a lake bottom contrasts with the simple plate case described above in two important respects. First, nodules are roughness elements that protrude from the bottom and, consequently, must modify the flow. There are no experimental data for the flow fields over disks on a surface. Schlichting (1968, p. 614) does report some measurements near spheres on a plane surface, but the relevance of these results to the present geometry is equivocal. Hypothetically, separation of the flow somewhere along the disk surface with the consequent development of secondary recirculating flows at the sides and rear is likely. Also, the leading edge of the nodule may not be hydrodynamically smooth and may engender its own local flows, all of which is quite speculative.

Yet, the object of this study is to advance a soluble model that can produce an order-of-magnitude correct estimate of the growth rate and the morphology of nodules. As such, I take the liberty to assume that nodules are sufficiently streamlined to allow the flow to conform to the nodule shape (fig. 2). This is arguably the most contentious assumption of the model.

The conformal-flow assumption will produce the desired results if the actual separation effects cause deviations in the mass transfer rates of no more than a factor of three over that predicted for smooth, conformal flow. Because there do not appear to exist any experimental studies of mass transport along surface-mounted discoidal/spheroidal

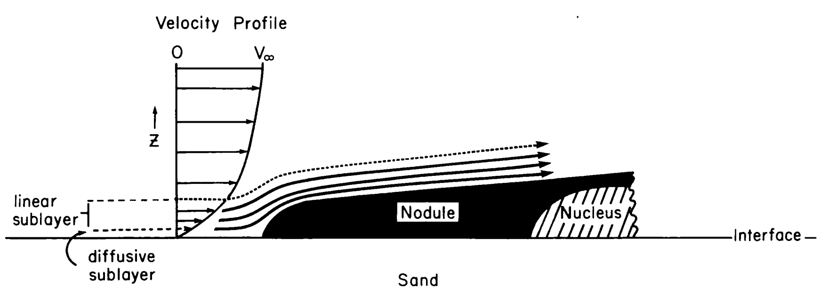

Fig. 2. Idealized flow over a nodule used in the quantitative calculation of the present model. The fluid flow is assumed conformal to the surface geometry. Likely complications such as stagnant zones, separation, and recirculation are ignored. The diffusive sublayer is buried well within the linear portion of the turbulent boundary layer and extends over the nodule surface.

objects, this last supposition cannot be verified exactly. Perturbations in the flow caused by a nodule can lead to both local decreases and increases in the mass-transfer rates. For example, flux measurements along the surface of spheres (Schutz, ms; Rhodes and Peebles, 1965) and cylinders (Lebouche and Martin, 1975) suspended in a turbulent free-stream indicate drops in mass-transfer rates in the zone of flow separation of no more than a factor of four. Conversely, there can be similar magnitude increases in these rates in the re-attachment zones behind wall-mounted ribs (for example, Berger and Hau, 1979). If these results represent extreme cases, then the conformal-flow results should be correct to within an order of magnitude.

In addition to the above, we can assert quite accurately that the growth of the nodule, in and of itself, does not perturb the flow, because the rate of growth of the nodule is so slow compared to the fluid-flow velocity that the flow can adjust easily to its changing shape.

Within the conformal boundary layer that envelops the nodule, the profile of the tangential velocity will obey eq (1) up to a distance of $u_* z/\nu \leq 7$ normal to the surface. The velocity profile in the conformal diffusive sublayer is therefore linear on a time-averaged basis (not laminar).

As a second profound difference, the nodule is assumed to be far more reactive as a sink for dissolved metals than the surrounding sand; the nodule-sand surface is not equally reactive, as was the flat plate, and eq (2) cannot be used to predict fluxes because the sublayer thickness is spatially variable.

Although a quantitative model for this situation is developed in the next section of this paper, it is instructive to present first a qualitative picture of the processes involved. As bottom waters approach a nodule lying on sand (fig. 3, point A), a dissolved metal profile in the vicinity of the bottom exhibits, at most, a weak gradient, because sand is neither a strong source nor a sink of metals. Upon reaching the leading edge of the nodule, the dissolved metal concentrations are those of the bottom water (fig. 3, point B).

As the water continues to flow over the nodule, gradients in metal concentrations develop in the fluid adjacent to the nodule surface due to removal by precipitation. A gradient is created because the water adjacent to the nodule is part of the diffusive sublayer in which relatively slow molecular diffusion dominates mass transport (Boudreau and Scott, 1978; Boudreau and Guinasso, 1982). The vertical extent of this gradient will propagate downstream, until it reaches the maximum allowed thickness of the diffusive sublayer, or the flow separates from the nodule, or the trailing edge of the nodule is encountered (Rosner, 1964; Petersen, 1965; Kader and Gukhman, 1977; Ghez, 1978). Consequently, dissolved metal concentrations at the nodule surface decrease progressively downstream (fig. 3, positions B–E).

The rate of Fe and Mn precipitation is a function of their concentrations in solution (for example, Stumm and Lee, 1961; Michard, 1969;

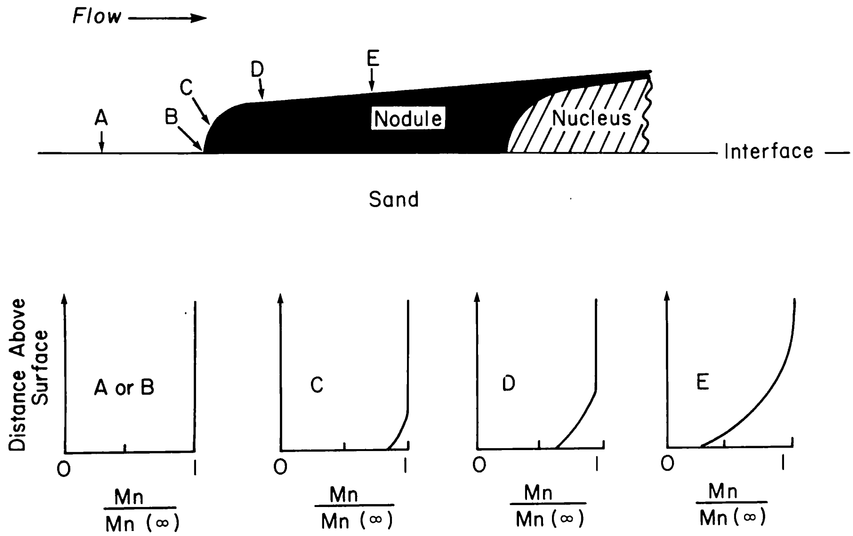

Fig. 3. Schematic representation of the development of a dissolved Mn gradient in the diffusive sublayer of water flowing over a discoidal nodule. Water approaching the nodules exhibits little or no metal gradient near the sediment-water interface (position A), because sand is a weak source or sink. At the leading edge (position B), the concentration at the nodule surface is essentially that of the bulk bottom water. As the water flows downstream along the nodule, dissolved Mn is removed from the water in contact with the nodule surface. A progressively thicker gradient develops, because slow molecular diffusion must replenish the Mn in the boundary layer (position C–E).

Hem, 1981; Chapnick, Moore, and Nealson, 1982; Diem and Stumm, 1984). Therefore, the rate of oxide deposition on the nodule surface drops downstream. So, as the leading-edge area grows faster, the nodule elongates with time in the direction of flow. (The spatial dependence of the flux to a reactive surface of finite extent has great relevance to the interpretation of alabaster dissolution experiments on the sea floor (Santschi and others, 1983). This aspect is discussed in the appendix.)

A pronounced elongation (that is to say, an apparent flattening) of a nodule requires that the concentration of dissolved metals at the nodule surface must decrease drastically downstream from the leading edge. This will be true only if the oxidation kinetics are rapid compared to the mean contact time of metal ions. I believe that the pseudo-homogeneous rate constants reported in the literature cannot be used to establish the validity of this presumption, because their conversion to true heterogeneous rate constants for a nodule surface is rife with questionable assumptions.

Nevertheless, the kinetics of metal precipitation onto lacustrine and neritic nodules are probably fast due to biological mediation (Callender and Bowser, 1976; Dean and Ghosh, 1981; Diem and Stumm, 1984). This is evidenced by the high rates of biogenic manganese-oxide deposition in water-supply pipelines cited by Tyler and Marshall (1967), that is, >10 mm yr^{-1}.

The preceding arguments explain the flattening of discoidal nodules, but what accounts for the near-radial symmetry? Again, the environmental growth conditions must be considered. Dean, Moore, and Nealson (1981) have found that the discoidal nodules of Lake Oneida, New York, are surprisingly mobile on the time scale of a year. (This observation is probably not unique to that lake but rather the *modus operandi* in the high-energy environment characteristic of sand accumulation.) Furthermore, current directions in shallow-water seas and lakes are highly variable on the time scale of an hour (P. LeBlond, personal commun.). Because of the relatively long growth time for nodules, that is, years (Manheim, 1965; Calvert and Price, 1977), compared to current variations and changes in orientation, a nodule should be subject to currents from all directions which, in turn, promote radial symmetry.

If the growth of lacustrine and neritic nodules found on coarse-grained sediments is primarily restricted to their upper surface and is controlled by the processes described above, then the lower surface of these nodules should exhibit truncated concentric bands due to natural variations and unevenness in growth. This type of structure can be seen in the photographs published by Sozanski and Cronan (1976, fig. 3).

MATHEMATICAL FORMULATION

A great advantage of the proposed theory is that it can be fashioned into an approximate mathematical model and tested by predicting growth rates to an accuracy of about a factor of three. The growth times of nodules are much longer than the time scale of water movement over nodules and replenishment of ions in the diffusive sublayer. Thus, the outward growth of a nodule can be treated as a pseudo-steady-state process. This mathematically decouples the growth of the nodule surface from the mass transport problem. Additionally, the nodule growth rate is sufficiently slow compared to the rate of rotation of the nodule relative to the flow that the spin rate can be assumed to be infinitely fast.

Choosing a coordinate system for this problem reveals immediately a fundamental difficulty with any attempt to solve this problem analytically. The flow field is easily represented in a Cartesian frame of reference, but the radially symmetric shape of the nodule proves to be awkward. Conversely, a cylindrical or polar coordinate system is well suited to the nodule morphology, but the flow field becomes unwieldy.

Again, a compromise must be made if a solution is to be realized. A numerical solution would surmount much of this problem, but this would require a great programming effort which is not justified by either the quality of the data or the stated aim of an order-of-magnitude correct solution. My approach has been to solve the problem as if each section across the nodule in the flow direction were part of an infinite strip (in the transverse direction). This is justified by the thinness of the diffusive sublayer compared to the radius of the nodule, except perhaps in the immediate vicinity of the nodule edge lateral to the flow. An attempt to correct for the rotation of the nodule is made later in this paper.

The time-averaged concentration field in the diffusive sublayer overlying the nodule surface is governed by (Kramers and Kreyger, 1956; Ling, 1963; Petersen, 1965; Kader and Gukhman, 1977; Ghez, 1978)

$$\frac{u_*^2 z}{\nu}\frac{\partial C}{\partial x} = D\frac{\partial^2 C}{\partial z^2} \tag{5}$$

where x ≡ coordinate in flow direction along the nodule surface ($x = 0$ at the leading edge), z ≡ coordinate normal to the surface, C ≡ concentration of precipitating metal in solution, u_* ≡ shear velocity, ν ≡ kinematic viscosity of water, and D ≡ molecular diffusion coefficient of the metal.

The eddy diffusivity, ϵ, which represents the time-averaged effects of the turbulence (bursts), is neglected in eq (5), because $\epsilon \ll D$ through most of the diffusive sublayer. As an illustration, Shaw and Hanratty (1977) give

$$\epsilon = 4.63 \cdot 10^{-4}\,\nu\left[\frac{u_* z}{\nu}\right]^{3.38} \qquad (z \to 0) \tag{6}$$

For the conditions cited below eq (4), $\delta = 0.0127$ cm. At this point, $\epsilon = 9.29 \cdot 10^{-6}\ \mathrm{cm^2\ sec^{-1}}$, which is comparable to $D = 5.75 \cdot 10^{-6}\ \mathrm{cm^2\ sec^{-1}}$; however, at $z = \delta/2$, ϵ has decreased precipitously to $8.98 \cdot 10^{-7}\ \mathrm{cm^2\ sec^{-1}}$. As the developing diffusive sublayer on the nodule surface reaches at most three-quarters of its maximum thickness, δ, neglect of ϵ is justified. In addition, the x-direction diffusion contributes negligibly (Apelblat, 1982) and is omitted from eq (5).

The sand surface surrounding the nodule is assumed chemically inert, while the nodule is assumed to be a first-order sink for metals (Michard, 1969; Hem, 1981).

$$D\frac{\partial C}{\partial z} = \begin{cases} 0 & (x < 0,\ z = 0) \quad \text{(sand)} \\ k\,C(x, 0) & (x \geq 0,\ z = 0) \quad \text{(nodule)} \end{cases} \tag{7}$$

where k ≡ heterogeneous rate constant. (If the reaction is biologically mediated, the rate constant, k, may not be a constant with position, x. The greater availability of dissolved metal at the leading edge may encourage a larger population near this point; k(x) would then decrease in magnitude toward the nodule center. This is an intriguing possibility, but it must be ignored for the moment due to its speculative nature.)

Inasmuch as the diffusive sublayer is buried within the viscous sublayer (Boudreau and Guinasso, 1982), and because the downstream growth of the gradient is unlikely to occupy all the diffusive sublayer, the boundary condition at the top of the sublayer is replaced by (Kader and Gukhman, 1977)

$$C\,(x, \infty) = C_\infty \tag{8}$$

where $C_\infty \equiv$ metal concentration measured in the bottom waters.

The solution of eqs (5) and (7) for the flux normal to the nodule surface along a line in the flow direction is (Apelblat, 1980)

$$D \frac{\partial C}{\partial z}\bigg|_{z=0} = \frac{3^{3/2}\,k\,C_\infty}{2\,\pi} \int_0^\infty \frac{e^{-(\gamma s)^3}}{1 + s + s^2}\,ds \tag{9}$$

where

$$\gamma \equiv \frac{k\,\Gamma\,(1/3)}{\Gamma\,(2/3)} \left[\frac{u_*^2 x}{3\nu D^2}\right]^{1/3} \tag{10}$$

and $\Gamma(\;) \equiv$ mathematical gamma function (Davis, 1964), and s is a dummy variable.

The instantaneous change in nodule thickness, r(x), at a point x′ along a line in the flow direction is

$$\frac{dr(x')}{dt} = \frac{D}{C_m(1 - \varphi)\rho} \frac{\partial C\,(x',z)}{\partial z}\bigg|_{z=0} \tag{11}$$

where $C_m \equiv$ Fe or Mn content of a nodule, $\rho \equiv$ nodule density (~2.5 g cm^{-3}), and φ is the porosity of the nodule (~0.4). The derivative in eq (11) is given by eq (9).

The solution given above is correct for any infinite strip across a stationary disk rather than a spinning disk. As explained below, no exact correction to the solution for the effects of rotation is possible. Fortunately, upper and lower bounds can be placed on the disk growth rates based on the strip results.

Consider first the correction along the leading edge of the nodule. With reference to figure 4, let $\overline{B'C'}$ be an (exaggerated) growth increment at the edge point B′ that is in the section that passes through the center, O, of the nodule. At any other point, B, on the leading edge, the growth vector in the flow direction is $\overline{BC} = \overline{B'C'}$, but the normal component of growth is the increment $\overline{AB}$, where $\overline{AB} = \overline{BC} \cdot \cos(\alpha)$, and $-\pi/2 \le \alpha \le \pi/2$. For a fast spinning nodule, the mean growth due to accretion on the leading edge is, therefore, smaller by a factor c_r,

$$c_r \equiv \frac{\int_{-\pi/2}^{\pi/2} \cos\alpha\, d\alpha}{\int_{-\pi/2}^{\pi/2} d\alpha} \tag{12A}$$

Along the trailing edge, the outward growth is also dependent on the angle α, but an exact value of this correction will not be needed.

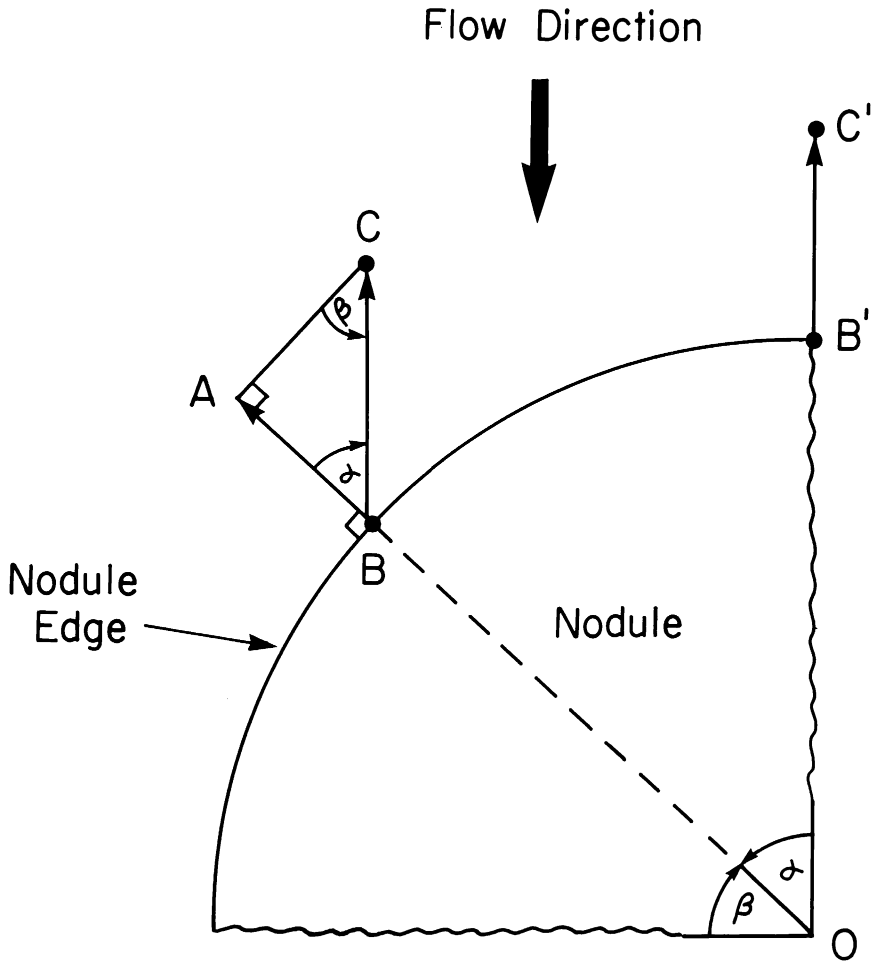

Fig. 4. Schematic illustration of the correction to the growth rate of the leading edge of a discoidal nodule. See the text for details.

Because of strong attenuation, significant growth is largely restricted to the vicinity of the leading edge. In fact, we shall find it useful to assume no growth on the trailing edge, so that the total correction at the nodule edge is

$$c_t \equiv \frac{\int_{-\pi/2}^{\pi/2} \cos\alpha \, d\alpha}{\int_0^{2\pi} d\alpha} = \frac{1}{\pi} \tag{12B}$$

At the center of the disk, point O, there is no correction, because this point is always in the same position relative to the flow. The correction for intervening points between the nodule edge and the center will fall monotonically between c_t and no correction. The precise value at an arbitrary radial position would require numerical solution of the problem. However, an upper limit to the growth time is obtained by assuming that the correction for the nodule edge, that is $1/\pi$, applies at all points. A lower limit to the time for growth is obtained by applying no correction at all.

In practice, the growth of a nodule is calculated by assuming an initial oxide deposit in the form of a small quarter sphere (<0.3 mm in radius) that would be attached to a nucleus. Thin layers of oxide (≤0.1 mm at the leading edge) are added successively with a thickness and on a time scale determined by eqs (9) and (11) to simulate nodule accretion. Because eq (11) is applied only at a finite number of points along the nodule surface, the actual surface of a nodule after an increment of growth is calculated by fitting a natural spline through the calculated points. The origin is shifted to the new leading edge after each growth increment. The apparent advection caused by the moving reference frame is negligibly small. The growth and fitting process are repeated to generate a complete nodule.

APPLICATION AND DISCUSSION

Eqs (9) and (11) dictate nodule growth-rate as a function of the environmental parameters C_∞ and u_* and of the physico-chemical parameters k, ν, and D. The parameters ν and D are essentially constant for the environments under consideration at $3.6 \cdot 10^5$ and 126 $cm^2\,yr^{-1}$, respectively. In addition, if sediment finer than sand is not to accumulate, then u_* must be $\geq 3.16 \cdot 10^7$ cm yr^{-1} (1 cm sec^{-1}; Miller and others, 1977).

Inspection of the solution, eq (9), shows that the leading edge, $\gamma = 0$, grows outward as a function of k and C_∞, but not u_*. The rate of deposition at points downstream, $\gamma > 0$, is a function of all three parameters; therefore, u_* does affect the nodule thickness but not its radius with time.

Values of k are not known and are not easily calculated from the pseudo-homogeneous rate constants determined for oxidation in sediments or in the water column. Be that as it may, the correct k-value must reproduce the observed ratio of the thickness of oxide at the center of a nodule (or at the nucleus) to the radius (the aspect ratio). The correct k-value can thus be determined by adjusting this parameter, until the observed aspect ratio is reproduced if all other parameter values are known.

The model was applied to simulate the formation of nodules under the conditions observed in Lake Charlotte. Manganese was treated as the controlling metal. Figure 5 illustrates the nodule surfaces generated with the edge correction applied at all points and for C_∞ = 1 ppm

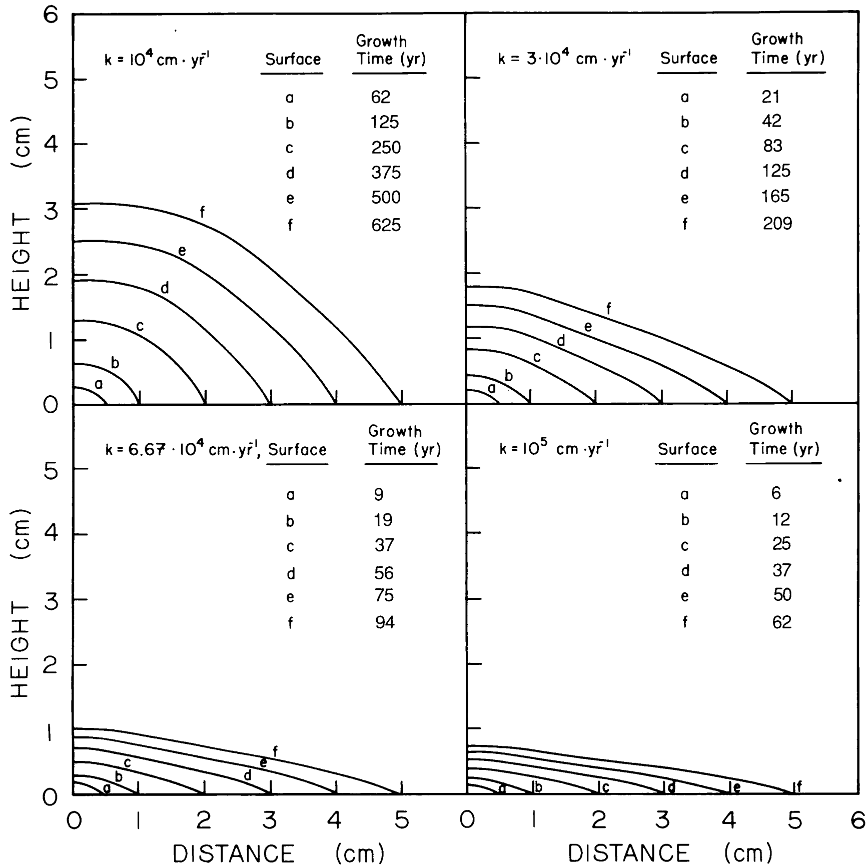

Fig. 5. Model predictions of the growth of the top surface of nodules lying on inert sand as a function of four different Mn precipitation constants, k, with bottom waters containing 1 ppm dissolved Mn and flowing with $u_* = 3.156 \cdot 10^7$ cm yr^{-1} (1.0 cm s^{-1}). The correction for the leading edge has been applied at all points. The origin marks the original center of the nucleus. In a real nodule, growth would be symmetric about this point. (The distance abscissa indicates the true distance from the center, not the x-coordinate taken along the nodule surface.)

(Kepkay, 1985), $C_m = 0.25$ (g·g^{-1}), and four different k-values. Note that the nodules elongate with increasing k, as expected. The aspect ratio for 5 cm nodules from Lake Charlotte is in the range of 1:5 to 1:10 (P. Kepkay, personal commun.). The theoretical k-values needed to produce such nodules are in the range 0.6 to $1.0 \cdot 10^5$ cm yr^{-1}.

The upper limit for the growth time of a 5 cm nodule in Lake Charlotte is about 100 yrs or a growth rate of 0.5 mm yr^{-1}. Because the growth correction is applied uniformly at all points, the lower limit is simply $1/\pi$ of this value or 32 yrs (1.7 mm yr^{-1}). This range is compatible with the growth rates estimated by Harris and Troup (1970) for nodules in Nova Scotia lakes by assuming that the internal bands are yearly growth rings; that is to say, 0.01 to 2.0 mm yr^{-1} (see also Kindle, 1935). It is also consistent with the minimum radiometric rates established by Dean and others (1981; >0.01 mm yr^{-1}) for nodules in Lake Oneida, New York.

As another application, the work of Grill (1978) indicates bottom-water manganese concentrations over a field of discoidal nodules in Jervis Inlet, British Columbia, of about 1 ppb. A scaling of the results of figure 5 to this concentration predicts growth-rates of about 0.5 to 2.0 mm kyr^{-1} for these nodules. This is in broad agreement with the radiometric rate determined by Ku and Glasby (1972) at this site, that is, >0.3 mm kyr^{-1}, and that calculated by Macdonald and Murray (1973), that is, ~3 mm kyr^{-1}.

The present model produces discoidal nodules on coarse-grained sediments not because of strong interstitial sources of metals, but because the nodule surface contrasts sharply with the surrounding sediment in reactivity to dissolved metals. Coarse-grained sediments appear to be weak sources or sinks of metals, while nodules efficiently scavenge manganese from solution. However, if the underlying sediment proves to be a source in some cases, the present theory would still suggest discoidal nodules, because a diagenetic contrast is present and, in fact, intensified. Only the details of the mathematical formulation of the model presented here need be modified.

This might also suggest that fine-grained sediments that are strong sources of Mn^{++} should produce discoidal nodules because the diagenetic contrast would be the most marked. However, spherical nodules are found normally on fine-grained sediments of lakes and shallow seas, because they appear to grow either from hydrodynamically more quiescent bottom waters or in stagnant interstitial waters (Calvert and Price, 1970).

The model can be extended to account for deep-sea nodule morphology. Oblate spheroidal nodules are reported from siliceous clays (Raab, 1972) which appear to be neither strong sources nor sinks of dissolved manganese (Klinkhammer, Heggie, and Graham, 1982). The bottom portion of these nodules may still accrete metals by a mechanism other than by classical remobilization (for example, Lyle, Heath, and Robbins, 1984), which does not detract from the present theory.

Deep-sea nodules resting on highly oxidized red clays are often spherical even though these sediments are not sources of dissolved Fe and Mn (Klinkhammer, 1980). This observation does not contradict the present theory. Deep-sea clays and shallow-water sands differ not only in grain size. Deep-sea clays contain appreciable amounts of oxide coatings that can act to remove dissolved metals from seawater in the same way as a nodule. In fact, nodules and sediments accumulate metals at very nearly the same rate (Bender, Ku, and Broecker, 1966). Because the relative contrast in reactivity of red clays and nodules is small, the present theory would suggest rounder nodules, if they are maintained at the interface. The mass-transfer model of Boudreau and Scott (1978) describes metal transport from seawater if there is no reactive contrast between sediment and nodule and correctly predicts the observed growth rates.

If the implied growth rate of Lake Charlotte nodules can be taken at face value, then an interesting correlation emerges. The growth-rates of lacustrine, marine shallow-water, and deep-sea nodules form a sequence that spans a factor of 10^5 to 10^6, that is, ~ 1, $\sim 10^{-3}$, and 10^{-5} to 10^{-6} mm yr^{-1}, respectively. The dissolved manganese in the overlying waters in these environments exhibits a similar trend, from 1 ppm in Lake Charlotte, to 10^{-3} ppm in Jervis Inlet, to something of the order of 10^{-5} ppm in the deep Pacific (Landing and Bruland, 1987).

This correlation is not perfect and may be quite fortuitous. Alternatively, it may be an expression of a fundamental reason for the observed differences in the growth rates of nodules from these different environments (spheroidal lacustrine nodules are excluded). If the precipitation of metals from the overlying waters is a major accretionary mechanism for nodules (or at least for their tops) and if this process is first order with respect to metal concentration, then, all else being constant, a linear correlation is required. (The correlation with dissolved Mn concentration becomes even tighter if the deep-sea rates are adjusted for the fact that abyssal mass-transfer coefficients are about an order of magnitude lower than those in shallow-water environments.)

CONCLUSIONS

The prominent discoidal shape of nodules from the bottoms of shallow seas and lakes is a result of the difference in the reactivity of the nodule surface relative to that of the surrounding sediment. Coarse-grained sediments are either weak sources or sinks, but nodules are relatively strong sinks.

Boundary-layer mass-transport theory can be combined with a simple kinetic scheme for oxide precipitation to generate an order-of-magnitude model for the nodule growth rates. Given a set of environmental parameters that characterize those observed in Lake Charlotte (Nova Scotia), the model reproduces both the general morphological features of the nodules found in this lake and predicts growth times that agree with independent estimates.

The rates of nodule growth in different environments (sandy bottoms of lakes, shallow-water seas, and the deep sea) appear to correlate linearly with the concentration of dissolved Mn in the bottom waters in contact with these nodules. This argues that bottom waters constitute an important source of metals for the growth of these nodules and that linear accretion kinetics are appropriate in modelling this process.

It is hoped that this paper will spur more effort into the determination of the growth rates of lacustrine and neritic nodules, the measurement of interstitial metal profiles and encourage flume studies of the flow around discoidal nodules and the precipitation of dissolved Mn onto these bodies. An accurate numerical simulation would then be justified.

ACKNOWLEDGMENTS

Earlier versions of this paper benefited greatly from comments by Steve Calvert, Mitchell Lyle, and Tom Pedersen. The Journal reviewers, Philippe Van Cappellen, Bill Casey, and James Ledwell, provided additional valuable criticism. This research was supported by grants #U0506 and #E0275 from the Natural Sciences and Engineering Research Council of Canada.

APPENDIX

On Alabaster Dissolution Experiments

The following calculations appeared originally in Boudreau (ms), but due to the general unavailability of this work, it was thought informative to repeat them here. In the meantime, similar calculations, as well as experimental verification, have been presented by Opdyke, Gust, and Ledivele (1987). Nonetheless, I have decided to retain this appendix, because it complements the development in the main text by offering additional proof of the utility of the present theory.

Santschi and others (1983) have attempted to measure the thickness of the diffusive sublayer on the deep-sea floor by studying the weight loss of an alabaster ($CaSO_4 \cdot 2H_2O$) plate placed semi-flush to the sediment-water interface. Assuming diffusion control of the dissolution and a mass transfer model of the form of eq (2), they calculated that the observed loss of material required a mean diffusive sublayer of 0.5 mm.

This figure would appear, however, to be a minimum estimate of the diffusive sublayer thickness at the sea-floor. First, they must assume that the plate, and particularly its leading edge, does not trip the flow to increase substantially the local amount of turbulence or that these disturbances have relaxed before the alabaster is reached. This is similar to my assumption that the flow over my discoidal nodule is streamlined.

If we grant this condition to be reasonably likely, then the extrapolation of the plate results to the sea floor is still flawed. There is no reason to believe that there is an appreciable gradient in $SO_4^=$ upstream of the plate. The diffusive sublayer for $SO_4^=$ begins at the leading edge of the alabaster and grows downstream, as it does for Mn on a discoidal nodule resting on sand. Therefore, their results represent an integration over a developing boundary layer and are not a true measure of the thickness of a fully developed diffusive sublayer on the adjacent sediment. This criticism can be verified by comparing their measured mean boundary-layer thickness to that predicted from a model for a spatially growing diffusive sublayer on a finite plate.

The kinetics of the alabaster dissolution reaction are assumed to be infinitely fast compared to the transport process (as did Santschi and his co-workers). Furthermore, the effects of lateral and back-diffusion are treated as insignificant. Then, the concentration of $SO_4^=$ in the diffusive sublayer is governed by eq (5) of the text (Kramers and Kreyger, 1956; Kader and Gukhman, 1977; Apelblat, 1980), subject to the boundary conditions,

$$C = C_{sw} \quad \text{as} \quad z \rightarrow \infty \tag{A1}$$

$$C = C_{sw} \quad \text{at} \quad z = 0, x < 0 \tag{A2}$$

$$C = C_{sat} \quad \text{at} \quad z = 0, x \geq 0 \tag{A3}$$

where C_{sw} is the concentration in the bulk flow, C_{sat} the saturation concentration, and $x = 0$ is the beginning of the plate.

A mathematically-identical problem was solved earlier by Leveque (1928) and more recently by Apelblat (1980). From this latter work, the pointwise thickness of the diffusive sublayer on the plate is

$$\delta = 1.857 \left[\frac{D\nu x}{u_*^2} \right]^{1/3} \tag{A4}$$

and the mean (integrated) thickness over the entire plate, x = 0 to "d", is

$$\bar{\delta} = 1.238 \left[\frac{D\nu d}{u_*^2} \right]^{1/3} \tag{A5}$$

The linear dimension "d" is not stated in Santschi and others (1983), but 10 cm is a reasonable guess based on their figure 2 (an underestimation of 5 cm would not alter the following conclusions). The shear velocity at their test station is likely to be about 0.1 cm sec^{-1}. Substitution of these values into eq (A5) produces a predicted sublayer thickness of 0.54 mm (with $\nu = 2 \cdot 10^{-2}$ cm^2 sec^{-1}, $D = 4 \cdot 10^{-6}$ cm^2 sec^{-1}, and $u_* = 0.1$ cm sec^{-1}). The agreement may be fortuitous, but it probably reflects a correct application of the theory.

If the alabaster plate underestimates the boundary-layer thickness, what is the correct value? The potential thickness can be calculated from eqs (3B) or (4) of the text along with the definition $\bar{\delta} \equiv D/\beta$. For the conditions noted above, this is 1.8 mm, and this value should be used in theoretical studies.

All the above assumes, of course, fast reaction kinetics. At low levels of saturation, the alabaster dissolution-reaction is likely to be first order (Barton and Wilde, 1971; Gorban and Miyamoto, 1985). Then, more accurate results can be obtained by using eq (9) of the text to calculate δ and $\bar{\delta}$. (Note that in the limit as $k \rightarrow \infty$, boundary condition (7) reduce to eqs (A2) and (A3), and eq (A5) is accurate.) It is possible for this reaciton to become second order (Gorban and Miyamoto, 1985), and a fully numerical solution would then be necessary.

References

Apelblat, A., 1980, Mass transfer with a chemical reaction of the first order: analytical solutions: Chem. Eng. Jour., v. 19, p. 9–37.

——— 1982, Mass transfer with a chemical reaction of the first order: Chem. Eng. Jour., v. 23, p. 193–203.

Barton, A. F. M., and Wilde, N. M., 1971, Dissolution rates of polycrystalline samples of gypsum and orthorhombic forms of calcium sulfate by a rotating disc method: Faraday Soc. Trans., v. 67, p. 3590–3597.

Bender, M. L., Ku, T. -L., and Broecker, W. S., 1966, Manganese nodules: their evolution: Science, v. 151, p. 325–328.

Berger, F. P., and Hau, K. -F. F. -L., 1979, Local mass/heat transfer distribution on surfaces roughened with small ribs: Internat. Jour. Heat Mass Transfer, v. 22, p. 1645–1656.

Blackwelder, R. F., and Haritonidis, J. H., 1983, Scaling of the bursting frequency in turbulent boundary layers: Jour. Fluid Mechanics, v. 132, p. 87–103.

Boudreau, B. P., ms, 1985, Diagenetic Models of Biological Processes in Aquatic Sediments: Ph.D. dissert., Yale Univ., New Haven, Conn., 526 p.

Boudreau, B. P., and Guinasso, N. L., 1982, The influence of a diffusive sublayer on accretion, dissolution, and diagenesis at the sea floor, *in* Fanning K. A., and Manheim, F. T., eds., The Dynamic Environment of the Ocean Floor: Lexington, Mass., Lexington Books., p. 115–145.

Boudreau, B. P., and Scott, M. R., 1978, A model for the diffusion-controlled growth of deep-sea manganese nodules: Am. Jour. Sci., v. 278, p. 903–929.

Callender, E., and Bowser, C. J., 1976, Freshwater ferromanganese deposits, *in* Wolf, K. H., ed., Handbook of Strata-Bound and Stratiform Ore Deposits: Amsterdam, Elsevier, p. 341–394.

Calvert, S. E., and Price, N. B., 1970, Composition of manganese nodules and manganese carbonates from Loch Fyne, Scotland: Contr. Mineralogy Petrology, v. 29, p. 215–233.

———1977, Shallow water, continental margin and lacustrine nodules: distribution and geochemistry, *in* Glasby, G. P., ed., Marine Manganese Deposits: Amsterdam, Elsevier, p. 45–86.

Campbell, J. A., and Hanratty, 1983a, Turbulent velocity fluctuations that control mass transfer to a solid boundary: Am. Inst. Chem. Eng. Jour., v. 29, p. 215–220.

———1983b, Mechanism of turbulent mass transfer at a solid boundary: Am. Inst. Chem. Eng. Jour., v. 29, p. 221–228.

Chapnick, S. D., Moore, W. S., and Nealson, K. H., 1982, Microbially mediated manganese oxidation in a freshwater lake: Limnology Oceanography, v. 27, p. 1004–1014.

Chriss, T. M., and Caldwell, D. R., 1984, Universal similarity and the thickness of the viscous sublayer at the ocean floor: Jour. Geophys. Research, v. 89, p. 6403–6414.

Corino, E. R., and Brodkey, R. S., 1969, A visual investigation of the wall region in turbulent flow: Jour. Fluid Mechanics, v. 37, p. 1–30.

Davies, J. T., 1977, Diffusion and heat transfer at the boundaries of turbulent liquids, *in* Spalding, D. B., ed., Physico-Chemical Hydrodynamics: London, Advance Pub., p. 3–22.

Davis, P. J, 1964, Gamma function and related functions, *in* Abramowitz, M., and Stegun, I. A., eds., Handbook of Mathematical Functions: New York, Dover, p. 253–293.

Dean, W. E., and Ghosh, S. K., 1981, Geochemistry of freshwater ferromanganese deposits in North America, *in* Grassely, G., ed., Geology and Geochemistry of Manganese, v. III.: Budapest, Akad. Kiado, p. 255–277.

Dean, W. E., Moore, W. S., and Nealson, K. H., 1981, Manganese cycles and the origin of manganese nodules, Oneida Lake, New York, U.S.A: Chem. Geology, v. 34, p. 53–64.

Deissler, R. G., 1951, Investigation of turbulent flow and heat transfer in smooth tubes, including the effects of variable fluid properties: Am. Soc. Mech. Eng. Trans., v. 73, p. 101–107.

Diem, D., and Stumm, W., 1984, Is dissolved Mn^{2+} being oxidized by O_2 in the absence of Mn-bacteria or surface catalysts?: Geochim. et Cosmochim. Acta, v. 48, p. 1571–1573

Fage, H., and Townsend, H. C. H., 1932, An examination of turbulent flow with an ultramicroscope: Royal Soc. Proc., v. A135, p. 656–677.

Ghez, R., 1978, Mass transport and surface reactions in Leveque's approximation: Internat. Jour. Heat Mass Transfer, v. 21, p. 745–750.

Gorban, G. R., and Miyamoto, S., 1985, Dissolution rate of gypsum in aqueous salt solutions: Soil Sci., v. 140, p. 89–93.

Grass, A. J., 1971, Structural features of turbulent flows over smooth and rough boundaries: Jour. Fluid Mechanics, v. 50, p. 233–255.

Grill, E. V., 1978, The effect of sediment-water exchange on manganese deposition and nodule growth in Jervis Inlet, British Columbia: Geochim. et Cosmochim. Acta, v. 42, p. 485–494.

Harris, R. C., and Troup, A. G., 1970, Chemistry and the origin of freshwater ferromanganese concretions: Limnology Oceanography, v. 15, p. 702–712.

Hem, J. D., 1981, Rates of manganese oxidation in aqueous systems: Geochim. et Cosmochim. Acta, v. 45, p. 1369–1374.

Hinze, J. O., 1975, Turbulence, 2d ed.: New York, McGraw-Hill, 790 p.

Kader, B. A., and Gukhman, A. A., 1977, Turbulent mass transfer with a first-order chemical reaction on the wall at $Pr \ll 1$: Internat. Jour. Heat Mass Transfer, v. 20, p. 1339–1350.

Kepkay, P. E., 1985, Kinetics of microbial manganese oxidation and trace metal binding in sediments: results from an *in situ* dialysis technique: Limnology Oceanography, v. 30, p. 713–726.

Kindle, E. M., 1935, Manganese concretions in Nova Scotia lakes: Royal Soc. Canada Trans., v. IV-29, p. 163–180.

Kline, S. J., Reynolds, W. C., Schraub, F. A., and Runstadler, P. W., 1967, The structure of turbulent boundary layers: Jour. Fluid Mechanics, v. 30 p. 741–773.

Klinkhammer, G. P., 1980, Early diagenesis in sediments from the eastern equatorial Pacific. II. Trace metal results: Earth Planetary Sci. Letters, v. 49, p. 81–101.

Klinkhammer, G. P., Heggie, D. T., and Graham, D. W., 1982, Metal diagenesis in oxic marine sediments: Earth Planetary Sci. Letters, v. 61, p. 211–219.

Kramers, H., and Kreyger, P. J., 1956, Mass transfer between a flat surface and a falling liquid film: Chem. Eng. Sci., v. 6, p. 42–48.

Ku, T.-L., and Glasby, G. P., 1972, Radiometric evidence for the rapid growth of shallow-water continental margin manganese nodules: Geochim. et Cosmochim. Acta, v. 36, p. 699–703.

Landing, W. M., and Bruland, K. W., 1987, The contrasting biogeochemistry of iron and manganese in the Pacific Ocean: Geochim. et Cosmochim. Acta, v. 51, p. 29–43.

Lebouche, M., and Martin, M., 1975, Convection forcee autour du cylindre: sensibilite aux pulsations de l'ecoulement externe: Internat. Jour. Heat Mass Transfer, v. 18, p. 1161–1175.

Leveque, M. A., 1928, Les lois de la transmission de chaleur par convection: Annals Mines, v. 13, p. 201–239.

Ling, S. C., 1963, Heat transfer from a small isothermal spanwise strip on an insulated boundary: Am. Soc. Mech. Eng. Trans., Jour. Heat Transfer, v. 85, p. 230–236.

Lyle, M., Heath, G. R., and Robbins, J. M., 1984, Transport and release of transition elements during early diagenesis: sequential leaching of sediments from MANOP Sites M and H. Part I. pH 5 acetic acid leach: Geochim. et Cosmochim. Acta, v. 48, p. 1705–1715.

Macdonald, R. D., and Murray, J. W., 1973, Sedimentation and manganese concretions in a British Columbia fiord (Jervis Inlet): Canada Geol. Survey Paper 73–23, 67 p.

Manheim, F. T., 1965, Manganese-iron accumulations in the shallow marine environment: Univ. Rhode Island, Narragansett Marine Lab., Occ. Pub. 3, p. 217–275.

Michard, G., 1969, Depot de traces de manganese par oxydation: Acad. Sci. Paris Comptes rendus, v. D269, p. 1811–1814.

Miller, M. C., McCave, I. N., and Komar, P. D., 1977, Threshold of sediment motion under unidirectional currents: Sedimentology, v. 24, p. 507–527.

Murray, J., and Irvine, R., 1894, On manganese oxides and manganese nodules in marine deposits: Royal Soc. Edinburgh Trans., v. 37, p. 721–742.

Opdyke, B. N., Gust, G., and Ledwell, J. R., 1987, Mass transfer from smooth alabaster surfaces in turbulent flow: Geophys. Research Letters, v. 14, p. 1131–1134.

Petersen, E. E. 1965. Chemical Reaction Analysis: Englewood Cliffs, N.J., Prentice-Hall, 276 p.

Price, N. B., 1967, Some geochemical observations on manganese-iron oxide nodules from different depth environments: Marine Geology, v. 5, p. 511–538.

Raab, W., 1972, Physical and chemical features of Pacific deep sea manganese nodules and their implications to the genesis of nodules, *in* Horn, D. R., ed., Ferromanganese Deposits on the Ocean Floor: Washington, Natl. Sci. Foundation, p. 31–49.

Rhodes, J. M., and Peebles, F. N., 1965, Local rates of mass transfer from spheres in ordered arrays: Am. Inst. Chem. Eng. Jour., v. 11, p. 481–487.

Rosner, D. E., 1964, Influence of the turbulent diffusive boundary layer on the apparent kinetics of surface catalyzed reactions in external flow systems: Chem. Eng. Sci., v. 19, p. 1–17.

Sandall, O. C., Hanna, O. T., and Mazet, P. R., 1980, A new theoretical formula for turbulent heat and mass transfer with gases or liquids in tube flow: Canadian Jour. Chem. Eng., v. 58, p. 443–447.

Santschi, P. H., Bower, P., Nyffeler, U. P., Azevedo, A., and Broecker, W. S., 1983, Estimates of the resistance to chemical transport posed by the deep-sea boundary-layer: Limnology Oceanography, v. 28, p. 899–912.

Schlichting, H., 1968, Boundary-layer Theory: New York, McGraw-Hill, 748 p.

Shaw, D. A., and Hanratty, T. J., 1977, Turbulent mass transfer rates to a wall for large Schmidt numbers: Am. Inst. Chem. Eng. Jour., v. 23, p. 28–37.

Sideman, S., and Pinczewski, W. V., 1975, Turbulent heat and mass transfer at interfaces: transport models and mechanisms, *in* Gutfinger, C., ed., Topics in Transport Phenomena: New York, John Wiley & Sons, p. 47–207.

Sozanski, A. G., and Cronan, D. S., 1976, Environmental differentiation of morphology of ferromanganese oxide concretion in Shebandowan Lakes, Ontario: Limnology Oceanography, v. 21, p. 894–898.

Stumm, W., and Lee, G. F. 1961, Oxygenation of ferrous iron: Indus. Eng. Chemistry, v. 53, p. 143–146.

Schutz, G., Ms, 1964, Die Messung lokaler Stoffubergangszahlen mit einer elektrochemischen Methode: Ph.D dissert. ETH, Zurich, Switzerland, 86 p.

Townsend, A. A., 1956, The Structure of Turbulent Shear Flow: Cambridge, Cambridge Univ. Press, 315 p.

Tyler, P. A., and Marshall, K. C., 1967, Microbial oxidation of manganese in hydroelectric pipelines: Antonie van Leeuwenhoek, v. 33, p. 171–183.

Varentsov, I. M., 1973, Geochemical aspects of formation of ferro-manganese ores in shelf regions of recent seas: Univ. Szegediensis, Acta Mineralogue-Petrographio, v. 21, p. 141–153.

Willmarth, W. W., and Sharma, L. K., 1984, Study of turbulent structure with hot wires smaller than the viscous length: Jour. Fluid Mechanics, v. 142, p. 121–149.

Winterhalter, B., 1981, Ferromanganese concretions in the Baltic Sea, *in* Grasselly, G., ed., Geology and Geochemistry of Manganese, v. III.: Budapest, Akad. Kiado, p. 227–254.